1908 *Chem. Mater.* **2010,** *22,* 1908–1914
DOI:10.1021/cm9036742

CHEMISTRY OF MATERIALS
Article

Symbiotic Coaxial Nanocables: Facile Synthesis and an Efficient and Elegant Morphological Solution to the Lithium Storage Problem

Fei-Fei Cao,[†,‡] Yu-Guo Guo,*[,†,‡] Shu-Fa Zheng,[†,‡] Xing-Long Wu,[†,‡] Ling-Yan Jiang,[†,‡] Rong-Rong Bi,[†,‡] Li-Jun Wan,*[,†,‡] and Joachim Maier*[,§]

[†]*Institute of Chemistry, Center for Molecular Sciences, Chinese Academy of Sciences* (*CAS*), [‡]*Beijing National Laboratory for Molecular Sciences* (*BNLMS*), *Beijing 100190, China, and* [§]*Max Planck Institute for Solid State Research, Heisenbergstrasse 1, 70569 Stuttgart, Germany*

Received December 7, 2009. Revised Manuscript Received January 6, 2010

Well-organized carbon nanotube (CNT)@TiO_2 core/porous-sheath coaxial nanocables are synthesized by controlled hydrolysis of tetrabutyl titanate in the presence of CNTs, and investigated with scanning electron microscopy, transmission electron microscopy, X-ray diffraction, and electrochemical experiments. The CNT@TiO_2 coaxial nanocables show excellent rate capability and cycling performance compared with both pure CNT and pure TiO_2 when used as anode materials for lithium-ion batteries (LIBs). Both the specific capacity in the CNT core and that in the TiO_2 sheath are much higher than that of the TiO_2-free CNT and that of the CNT-free TiO_2 sample, respectively. These results demonstrate that the coaxial cable morphology provides a clever solution to the ionic-electronic wiring problem in LIBs as well as the synergism of the two cable wall materials. On one hand, the CNT core provides sufficient electrons for the storage of Li in TiO_2 sheath. On the other hand, the CNT itself can also store Li whereby this storage kinetics is, in turn, improved by the presence of the nanoporous TiO_2 because the only very thin protection layer on TiO_2 (unlike free CNT) enables rapid access of Li-ions from the liquid electrolyte. This fascinating symbiotic behavior and the fact that the cable morphology leads to an efficient use of this symbiosis makes this solution match the requirements of LIBs extremely well.

Introduction

There is no doubt about the significance of Li-based batteries for our future lives, yet there is also no doubt about the necessity of finding better electrode materials.[1−11] Materials are needed that fulfill the harsh and often conflicting requirements to store high amounts of lithium and to do so rapidly and reversibly, let alone other decisive criteria such as low weight, low volume, environmental benignity, and last but not least low cost.[12−15] This means demanding too much of a single component, and one has to search for clever composite and morphological solutions. Here we present an efficient and elegant solution that consists in preparing coaxial nanocables based on carbon nanotubes enveloped by a nanoporous TiO_2 sheath. While the carbon nanotubes assist the storage in TiO_2 by providing electrons, the nanoporous TiO_2 sheath assists the storage in the carbon nanotubes by enabling rapid access of Li^+ from the liquid electrolyte. As the roles of ions and electrons are very different but complementing (compare acid−base activity with redox activity), the mutually beneficial role of the two intimately connected components TiO_2 (providing Li^+ for CNT) and CNT (providing electrons for TiO_2) finds a picturesque metaphor in the Chinese yin-yang principle.[16,17]

A key problem in Li-battery research is guaranteeing sufficiently rapid transport of both ions and

*Corresponding author. E-mail: ygguo@iccas.ac.cn (Y.-G.G.); wanlijun@iccas.ac.cn (L.-J.W.); s.weiglein@fkf.mpg.de (J.M.).

(1) Armand, M.; Tarascon, J. M. *Nature* **2008**, *451*, 652–657.
(2) Tarascon, J. M.; Armand, M. *Nature* **2001**, *414*, 359–367.
(3) Arico, A. S.; Bruce, P.; Scrosati, B.; Tarascon, J. M.; Van Schalkwijk, W. *Nat. Mater.* **2005**, *4*, 366–377.
(4) Poizot, P.; Laruelle, S.; Grugeon, S.; Dupont, L.; Tarascon, J. M. *Nature* **2000**, *407*, 496–499.
(5) Maier, J. *Nat. Mater.* **2005**, *4*, 805–815.
(6) Kang, K. S.; Meng, Y. S.; Breger, J.; Grey, C. P.; Ceder, G. *Science* **2006**, *311*, 977–980.
(7) Whittingham, M. S. *Dalton Trans.* **2008**, 5424–5431.
(8) Chung, S. Y.; Bloking, J. T.; Chiang, Y. M. *Nat. Mater.* **2002**, *1*, 123–128.
(9) Sun, Y.-K.; Myung, S.-T.; Park, B.-C.; Prakash, J.; Belharouak, I.; Amine, K. *Nat. Mater.* **2009**, *8*, 320–324.
(10) Kang, B.; Ceder, G. *Nature* **2009**, *458*, 190–193.
(11) Islam, M. S.; Driscoll, D. J.; Fisher, C. A. J.; Slater, P. R. **2005**, *17*, 5085−5092.
(12) Ellis, B. L.; Makahnouk, W. R. M.; Makimura, Y.; Toghill, K.; Nazar, L. F. *Nat. Mater.* **2007**, *6*, 749–753.
(13) Dominko, R.; Bele, M.; Goupil, J. M.; Gaberscek, M.; Hanzel, D.; Arcon, I.; Jamnik, J. *Chem. Mater.* **2007**, *19*, 2960–2969.
(14) Ng, S. H.; Wang, J. Z.; Wexler, D.; Konstantinov, K.; Guo, Z. P.; Liu, H. K. *Angew. Chem., Int. Ed.* **2006**, *45*, 6896–6899.
(15) Odani, A.; Pol, V. G.; Pol, S. V.; Koltypin, M.; Gedanken, A.; Aurbach, D. *Adv. Mater.* **2006**, *18*, 1431–1436.
(16) Jiang, L.; Wang, R.; Yang, B.; Li, T. J.; Tryk, D. A.; Fujishima, A.; Hashimoto, K.; Zhu, D. B. In *1st IUPAC Workshop on Advanced Material* (*WAM1*); Hong Kong, P. R. China, July 14−18, 1999; International Union for Pure Applied Chemistry: Research Triangle Park, NC, 2000; pp 73−81.
(17) Sun, T.; Wang, G.; Feng, L.; Liu, B.; Ma, Y.; Jiang, L.; Zhu, D. *Angew. Chem., Int. Ed.* **2004**, *43*, 357–360.

 Published on Web 01/22/2010

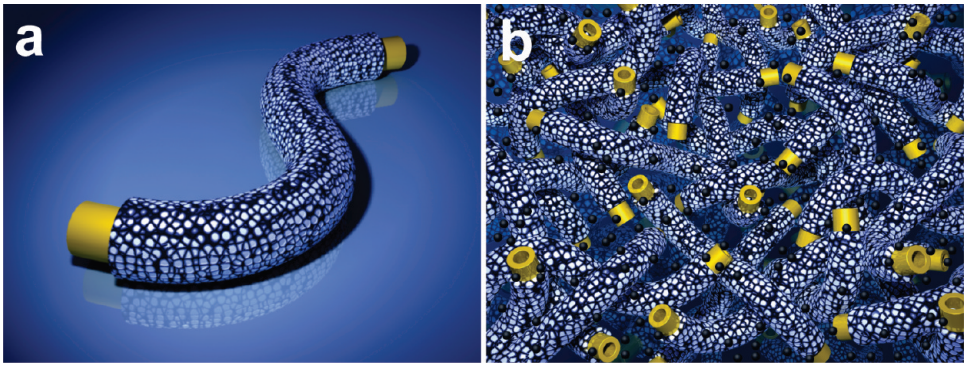

Figure 1. Symbiotic coaxial nanocables. (a) Schematic illustration of symbiotic coaxial nanocables with electronically conducting core (e.g., CNTs) and Li^+ providing nanoporous sheath (e.g., TiO_2). (b) Corresponding schematic illustration of the effectively mixed conducting 3D networks formed by the nanocables and carbon black.

electrons.[18−25] Only a few exceptional materials (such as Ag_2S) provide fast ionic and electronic conduction even at room temperature that is sufficient to enable rapid chemical transport even in big crystals. Many more materials, such as carbon, provide sufficient electronic conductivity but lack of sufficient ion conductivity. Here an appropriate solution is the preparation of nanoporous carbon structures (or even better, hierarchically porous carbon structures) in which then the ionic path is provided by the liquid electrolyte penetrating into the pores.[26] The diffusion length of the active material is now determined by the distances between the pores. As it is of nano size the diffusion time is−in spite of the low intrinsic diffusion coefficients−negligible.[5,27] In such cases, the ion transfer through the solid electrolyte interphase (SEI) is still a problem. After all, the necessary mixed conduction (Li^+ and e^-) is provided by the heterogeneous network. The same principle of "effectively mixed conducting materials" can be extended to materials in which now both electronic and ionic transport is poor.[28] It was shown that excellent properties can then be attained by not only nanostructuring it but by providing metallization of the pores.[19,20] To become commercially viable, a cost-effective coating material is desired to replace the expensive RuO_2 used in refs 19 and 20 for such nanostructures. One contribution to solve the problem is the use of a 3D current collector network of Cu nanorods,[29] which leads to much enhanced power performance but is naturally not meant for achieving high energy demands because of the limitation of the electrode thickness, which is determined by the length of the Cu nanorods fabricated by template-synthesis method. Carbon nanotube (CNT) is one of the best materials choices in views of facile fabrication and high electronic conductivity. CNT is also a fine Li-storage host as well as a fast Li insertion−extraction host at a low voltage, which makes it an attractive anode material for lithium-ion batteries.[30] However, the practical applications suffer from a high level of irreversibility (low columbic efficiency) and poor cycle life because of the pronounced surface reactions between CNTs and electrolyte.

The basic point in our paper is the mutually beneficial, i.e., symbiotic, role of the two intimately connected phases CNT and TiO_2. CNT is not just a metallizer for the storage material TiO_2, it efficiently stores Li as well. In turn, for the storage of Li in CNT, the TiO_2 proves helpful, too. It allows for a rapid access of ions to the CNT. As a consequence, the storage properties (as shown below) are superior to those of both individual constituents. To stress it again: The storage of TiO_2 is improved by the contact with CNT and, even more remarkably, the storage in CNT is improved by the presence of TiO_2. There are not very many morphological solutions one can think of to realize this concept. One possibility could be bilayers of carbon and titania immersed in the liquid electrolyte. This is though a rather academic play of thoughts. An optimum solution indeed is the nanocable network presented here (see Figure 1). It is not only elegant, its realization is facile and it offers excellent properties. A very favorable point consists in the fact that the tips of the cables are carbon-terminated (see Figure 2c), enabling necessary electronic percolation. To contact these tips, we admix carbon black on a micrometer scale, as shown in Figure 1b. In this way, two effectively mixed conducting networks are established, one on the nano, the other on the microscale.

(18) Derrien, G.; Hassoun, J.; Panero, S.; Scrosati, B. *Adv. Mater.* **2007**, *19*, 2336–2340.
(19) Guo, Y. G.; Hu, Y. S.; Sigle, W.; Maier, J. *Adv. Mater.* **2007**, *19*, 2087–2091.
(20) Hu, Y. S.; Guo, Y. G.; Dominko, R.; Gaberscek, M.; Jamnik, J.; Maier, J. *Adv. Mater.* **2007**, *19*, 1963–1966.
(21) Park, K. S.; Schougaard, S. B.; Goodenough, J. B. *Adv. Mater.* **2007**, *19*, 848–851.
(22) Singhal, A.; Skandan, G.; Amatucci, G.; Badway, F.; Ye, N.; Manthiram, A.; Ye, H.; Xu, J. J. *J. Power Sources* **2004**, *129*, 38–44.
(23) Herle, P. S.; Ellis, B.; Coombs, N.; Nazar, L. F. *Nat. Mater.* **2004**, *3*, 147–152.
(24) Hu, Y. S.; Liu, X.; Muller, J. O.; Schlogl, R.; Maier, J.; Su, D. S. *Angew. Chem., Int. Ed.* **2009**, *48*, 210–214.
(25) Wang, D. H.; Choi, D. W.; Li, J.; Yang, Z. G.; Nie, Z. M.; Kou, R.; Hu, D. H.; Wang, C. M.; Saraf, L. V.; Zhang, J. G.; Aksay, I. A.; Liu, J. *ACS Nano* **2009**, *3*, 907–914.
(26) Hu, Y. S.; Adelhelm, P.; Smarsly, B. M.; Hore, S.; Antonietti, M.; Maier, J. *Adv. Funct. Mater.* **2007**, *17*, 1873–1878.
(27) Maier, J. *J. Power Sources* **2006**, 569–574.
(28) Guo, Y. G.; Hu, J. S.; Wan, L. *J. Adv. Mater.* **2008**, *20*, 2878–2887.
(29) Taberna, L.; Mitra, S.; Poizot, P.; Simon, P.; Tarascon, J. M. *Nat. Mater.* **2006**, *5*, 567–573.
(30) Odani, A.; Nimberger, A.; Markovsky, B.; Sominski, E.; Levi, E.; Kumar, V. G.; Motiei, A.; Gedanken, A.; Dan, P.; Aurbach, D. In *11th International Meeting on Lithium Batteries*; Monterey, CA, June 22−28, 2002; Elsevier Science BV: Amsterdam, 2002, p 517−521.

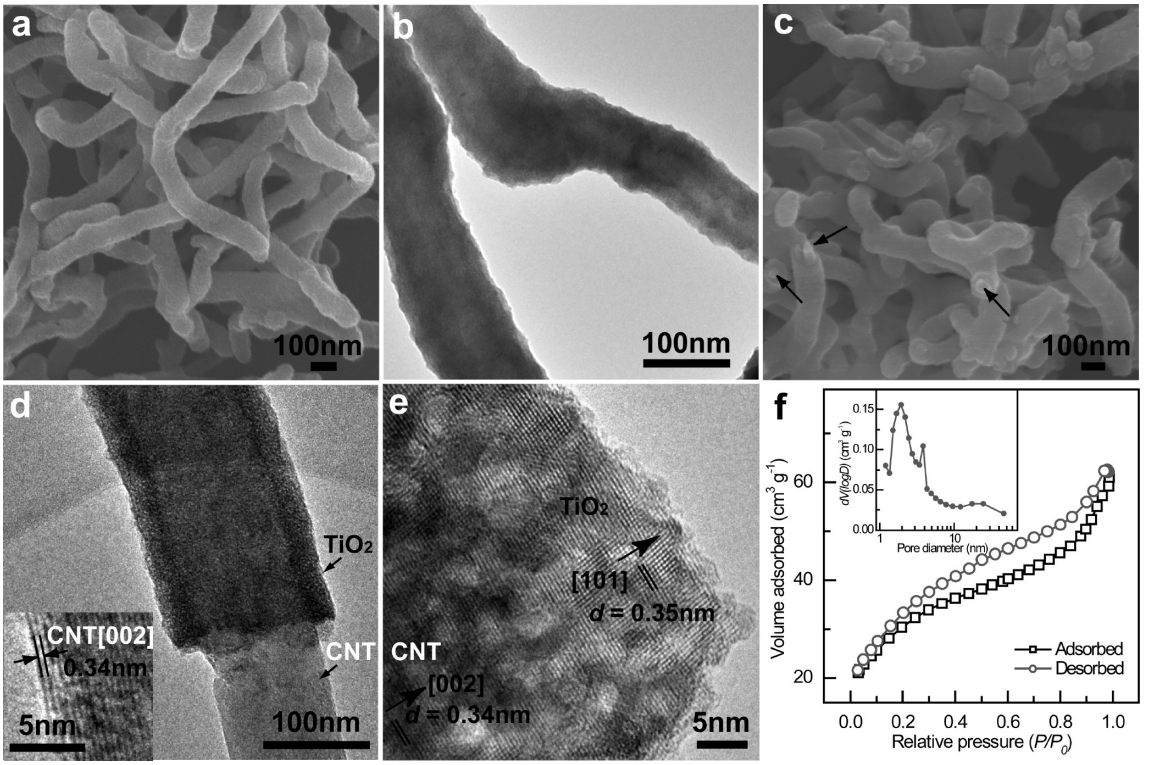

Figure 2. Morphology and structure. (a) SEM and (b) TEM images of TiO_2-precursor coated CNTs. (c) SEM and (d, e) HRTEM images of CNT@TiO_2 nanocables. (f) Nitrogen adsorption/desorption isotherms of CNT@TiO_2 nanocables, inset shows the pore size distribution plot which was calculated according to the BJH formalism.

Experimental section

Synthesis of CNT@TiO_2 Coaxial Nanocables. All the reagents were of analytical grade purity and were used as received. Multiwalled carbon nanotubes (MWCNTs, Shenzhen Nanotech Port Co. Ltd.) were refluxed in 6 M HNO_3 solution to remove any impurity and to oxidize the opened end of tubes, thereby making them more dispersible in ethanol. In a typical synthesis, twenty milligrams of the acid-treated CNTs were ultrasonically dispersed in 60 mL of ethanol for 5 h. Then 400 μL tetrabutyl titanate was added and the mixture was magnetically stirred for 30 min followed by the addition of 400 μL H_2O. After being further stirred for 30 min, the mixture was refluxed at 100 °C for 6 h. After the reaction, the suspension and precipitate were separated by centrifugation, washed with ethanol three times, and then dried at 80 °C. The as-prepared TiO_2-precursor coated CNTs were calcined at 400 °C under Ar for 4 h to obtain crystalline CNT@TiO_2 coaxial nanocables.

Structure and Morphology Characterization. The products were characterized by SEM (JEOL 6701F) and TEM (JEM JEOL 2010). All SEM and TEM samples of active materials in the lithiated/delithiated state were prepared in an argon-filled glovebox, washed three times with dimethyl carbonate (DMC), and sealed in an argon-filled jar before characterization. The XRD patterns were obtained by a Rigaku D/max-2500 using filtered Cu Kα radiation. The nitrogen adsorption and desorption isotherms at 77.3 K were obtained with a Nova 2000e Surface Area-Pore Size Analyzer. TGA was carried out using a Diamond TG-DTA Perkin-Elmer-SII instruments under air from 310 to 1300 K.

Electrochemical Characterization. Electrochemical experiments were performed using Swagelok-type cells assembled in an argon-filled glovebox. For preparing working electrodes, a mixture of CNT@TiO_2 nanocables, super-P acetylene black, and poly(vinyl difluoride) (PVDF) at a weight ratio of 80:10:10 was pasted on a Cu foil. The loading mass of active materials is about 10 mg cm^{-2}. A glass fiber (GF/D) from Whatman was used as a separator. Lithium foil was used as the counter electrode. The electrolyte consisted of a solution of 1 M $LiPF_6$ in ethylene carbonate (EC)/dimethyl carbonate (DMC)/diethyl carbonate (DEC) (1:1:1, in wt %) obtained from Novolyte Technologies. Galvanostatic cycling tests of the assembled cells were carried out on an Arbin BT2000 system in the voltage range of 0.01− 3.0 V and 1−3 V (vs Li^+/Li) under different current densities.

Results and Discussion

Integrating CNTs into functional architectures and composites has become an active research field because of potential application fields such as catalysis, chemical sensing, or energy research.[31,32] However, controllable self-assembly of nanoporous building blocks is still a challenge. We developed a facile wet-chemical synthetic route to deposit nanoporous TiO_2 onto CNTs. Well-organized CNT@TiO_2 core/porous-sheath coaxial nanocables were successfully synthesized by controlled hydrolysis of tetrabutyl titanate (TBT) in the presence of CNTs. Though there are many publications concerning oxide/CNT composites, most of them focus on the preparation and the applications other than lithium storage. Among them two very recent independent works need to be mentioned in which similar morphologies have

(31) Moriguchi, I.; Hidaka, R.; Yamada, H.; Kudo, T.; Murakami, H.; Nakashima, N. *Adv. Mater.* **2006**, *18*, 69–73.
(32) Woan, K.; Pyrgiotakis, G.; Sigmund, W. *Adv. Mater.* **2009**, *21*, 2233–2239.

been obtained. One refers to TiO_2/CNT cable structures that were prepared for improving photocatalytic properties.[32] There, the TiO_2 sheath is dense and would not be helpful in our context. The second one refers to MnO_2/CNT cable structures that are measured for Li battery electrodes, also with a dense oxide sheath.[33] Both papers do not show a symbiotic effect toward fast lithium storage, as explained in more detailed below.

Bearing in mind that the surface property of CNTs is the key factor in controlling morphology, by acting on the nucleation of deposits through certain interaction with metal ions, we treated as-received CNTs with strong acid, here 6 M HNO_3, to create functional oxygenated groups on their surfaces.[34] The acid treatment does not change the morphology and crystalline structure of multiwalled CNTs (see the Supporting Information, Figure S1−4) but is helpful for a better dispersion of CNTs in ethanol as well as better interfacial adhesion between deposited sheath and CNTs, and thus favors homogeneous TiO_2 deposition. Another key point in controlling assembly of TiO_2 is the proper hydrolysis kinetics of TBT. We found that this could be achieved by simply adding some water into the ethanol solution. In a typical synthesis, an optimized H_2O volume of 200 μL is added to 30 mL of ethanol solution containing 10 mg of CNTs and 200 μL of TBT for depositing a uniform coating layer of TiO_2 precursor on CNTs (see the Supporting Information, Table S1 and Figure S5). A lesser amount of H_2O resulted in thin and irregular coating layers, whereas a greater amount led to significant aggregation of CNTs. In addition, for a continuous growth of deposits (favorable coating layers of TiO_2 precursor), a well-adjusted TBT to CNTs ratio is crucial. Hereafter, we discuss only the samples prepared from the optimized system (Sample O1 in the Supporting Information, Table S1) with a weight ratio of 20:1 for TBT to CNTs and a volume ratio of 1:150 for H_2O to ethanol.

Figure 2a shows a typical scanning electron microscopy (SEM) image of CNTs after the coating process. The nanotubes in Figure 2a appear to have smooth surfaces with an average diameter of ca. 150 nm, whereas the initial CNTs have a small diameter ranging from 50 to 100 nm. It indicates that the precursor layer has successfully coated the CNTs. Further evidence can be found from transmission electron microscopy (TEM) image, as shown in Figure 2b, in which a uniform coating layer can be clearly seen. The TiO_2 precursor coated nanotubes were subsequently calcined under Ar atmosphere at 400 °C to prepare CNT@ TiO_2 core/sheath coaxial nanocables. The morphologies of the nanotubes are well maintained after calcining, although the surfaces of the nanotubes become slightly rough (Figure 2c). The feature of the core/sheath nanocable structure is revealed in the broken tips of nanocables in the SEM image (Figure 2c, indicated by arrows). Further evidence for the core/sheath structure can be found from the high resolution transmission electron microscopy (HRTEM) image of a broken nanocable shown in Figure 2d. A uniform sheath with a thickness of about 25 nm can be clearly seen in the image. The 0.34 nm spacing observed in the core of the coaxial nanocable corresponds to the (002) crystalline planes of the muliti-walled CNTs (inset in Figure 2d). In a HRTEM image taken from the edge of the nanocable (Figure 2e), the lattice fringes are clearly visible with a spacing of 0.35 nm, which is in good agreement with the spacing of the (101) planes of anatase TiO_2, thus demonstrating the presence of nanocrystalline TiO_2. Figure S3d in the Supporting Information shows the X-ray diffraction (XRD) pattern of the nanocables, in which all the diffraction peaks appeared after coating are in good agreement with anatase TiO_2 (space group $I4_1/amd$ (No. 141)) with lattice constants $a = b = 3.7852$ Å and $c = 9.5139$ Å (JCPDS No.21−1272), thus confirming the successful growth of the outer sheath of anatase TiO_2.[35] The corresponding Raman spectrum of the CNT@TiO_2 coaxial nanocables shows five Raman modes with strong intensities at 149, 199, 391, 509, and 627 cm^{-1} (see the Supporting Information, Figure S4d), which are consistent with the typical Raman features of anatase TiO_2 phase and also confirm the anatase phase of the outer sheath of TiO_2.[36] The HRTEM image in Figure 2e reveals the highly nanoporous structure of the TiO_2 sheath. Many nanopores in size ranging from 1 to 3 nm well dispersed in the entire sheath layer are clearly observable in the image. Not only is the pore structure three-dimensionally interconnected but the sheath also exhibits a three-dimensionally interconnected framework made up of nanosized building blocks—anatase nanograins—with an average size of about 5 nm. These nanopores are one key for an easy access of Li^+ from the liquid electrolyte for lithium storage in the CNT cores, the other is the small thickness of the passivation layer as described below. It is worth noting that the TiO_2 nanograins prefer to grow in a coherent manner on the CNT surfaces with a preferred ⟨101⟩ orientation along the ⟨001⟩ direction of CNTs (Figure 2e). To further investigate the pore structure of the sample, nitrogen isothermal adsorption technique was used. Figure 2f shows adsorption/desorption isotherms that exhibit a hysteresis typical of a nanoporous system. According to Brunauer−Emmett−Teller (BET) analysis, a total specific surface area of 110 $m^2\ g^{-1}$ is obtained for the CNT@TiO_2 nanocables, which is much larger than that of the acid-treated CNTs without coating layers (70 $m^2\ g^{-1}$) and that of the initial CNTs (61 $m^2\ g^{-1}$). This arises primarily from the formation of nanoporous TiO_2 sheath. The Barrett−Joyner−Halenda (BJH) pore size distribution (inset in Figure 2f) indicates that the CNT@TiO_2 nanocables exhibit three types of pores with different average diameters of 2.0, 3.8, and 24.5 nm. The 2.0 nm pores are resulting from the nanoporous TiO_2 sheath, which is consistent with the above HRTEM

(33) Reddy, A. L. M.; Shaijumon, M. M.; Gowda, S. R.; Ajayan, P. M. *Nano Lett*. **2009**, *9*, 1002–1006.
(34) Zheng, S. F.; Hu, J. S.; Zhong, L. S.; Song, W. G.; Wan, L. J.; Guo, Y. G. *Chem. Mater*. **2008**, *20*, 3617–3622.
(35) Guo, Y. G.; Hu, Y. S.; Maier, J. *Chem. Commun*. **2006**, 2783–2785.
(36) Miao, Z.; Xu, D.; Ouyang, J.; Guo, G.; Zhao, X.; Tang, Y. *Nano Lett*. **2002**, *2*, 717–720.

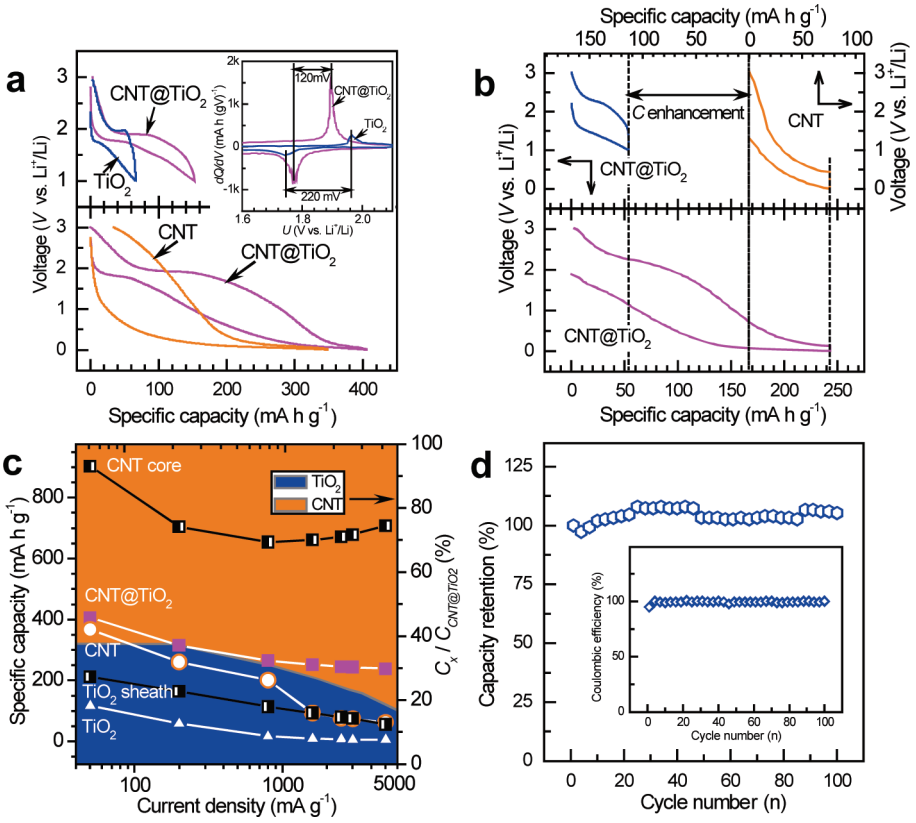

Figure 3. Lithium-storage properties. The typical discharge−charge profiles of CNT@TiO_2, TiO_2-free CNT, and CNT-free TiO_2 sample under current densities of (a) 50 and (b) 3000 mA g^{-1} between voltage limits of 1−3 and 0.01−3 V. The inset in (a) shows the corresponding differential capacity plots. (c) Comparison of the rate performance of CNT@TiO_2, TiO_2-free CNT, and CNT-free TiO_2 sample between voltage limits of 0.01−3 V. The specific storage capacities in CNT core and TiO_2 sheath are also shown. Shaded areas represent the capacity contribution from TiO_2 or CNT in the CNT@TiO_2 nanocables. (d) Cycling performance of CNT@TiO_2 nanocables under a current density of 1000 mA g^{-1} between voltage limits of 0.01−3 V. The inset shows the corresponding Coulombic efficiency profiles.

observation, whereas the 3.8 nm pores should be attributed to CNTs as confirmed by BJH results of both CNTs and acid-treated CNTs (see the Supporting Information, Figure S6). The large pores with sizes ranging from 10 to 90 nm are interspaced pores among nanotubes or nanocables in view of the existence in all of the three samples. Thermogravimetric analysis (TGA) was used to determine the chemical composition of the final nanocables (see the Supporting Information, Figure S7). The result shows that the nanocomposites have a chemical composition of 72 wt % TiO_2 and 28 wt % CNTs.

Figure 3a displays the typical discharge/charge profiles of the CNT@TiO_2 nanocables cycled under a current density of 50 mA g^{-1} between the voltage limits of 1−3 V and 0.01−3 V vs Li^+/Li, respectively. For comparison, the TiO_2 sample, which was synthesized in a control experiment in the absence of CNTs (see the Supporting Information, Figures S8 and S9), and acid-treated CNTs were also tested. Since the Li storage in CNT is mainly occurring below 1 V (Figures 3a and 3b), and the reversible Li storage in TiO_2 is usually reported between 1 and 3 V,[37−39] the storage in CNT@TiO_2 can be approximately decomposed into a storage into TiO_2 (occurring between 1 and 3 V) and a storage into CNT (<1 V). Both of them show much greater specific storage values. The reversible Li storage in the mesoporous TiO_2 sheath of CNT@TiO_2 is up to $Li_{0.63}TiO_2$ (i.e., 212 mA h g^{-1} based on the mass of TiO_2 in the composite). The value is much larger than that of the CNTs-free sample (ca. 66 mA h g^{-1}) and well comparable with the best results obtained for nanostructured TiO_2[19,35,37−39] for which a good electronic wiring is a necessary condition. The high lithium storage capability should be ascribed to the improved kinetics of the TiO_2 sheath benefiting from the high electronically conductive core of CNT, which is confirmed by the much lower polarization of the CNT@TiO_2 (ca. 120 mV) than that of the CNTs free sample (ca. 220 mV) (inset in Figure 3a).

A total reversible capacity (per total mass) of about 406 mA h g^{-1} in the voltage range of 0.01−3 V was obtained for the CNT@TiO_2 nanocables under a current density of 50 mA g^{-1}, which is larger than that of the acid-treated CNTs (ca. 367 mA h g^{-1}) at the same experimental condition. An even more remarkable performance was found when the samples were cycled using a higher current density. For example, at a current density of as much as 3000 mA g^{-1} (Figure 3b), CNT@TiO_2 can still deliver a specific capacity of 244 mA h g^{-1} between the voltage limits of 0.01 and 3 V, whereas the CNTs without

(37) Reiman, K. H.; Brace, K. M.; Gordon-Smith, T. J.; Nandhakumar, I.; Attard, G. S.; Owen, J. R. *Electrochem. Commun.* **2006**, *8*, 517–522.
(38) Armstrong, A. R.; Armstrong, G.; Canales, J.; Garcia, R.; Bruce, P. G. *Adv. Mater.* **2005**, *17*, 862–865.
(39) Wang, K. X.; Wei, M. D.; Morris, M. A.; Zhou, H. S.; Holmes, J. D. *Adv. Mater.* **2007**, *19*, 3016–3020.

TiO_2 coating layers have only 74 mA h g^{-1}, and the CNT-free TiO_2 nearly has no capacity under these conditions (see the Supporting Information, Figures S10). The results clearly indicate that the sheer presence of the outside TiO_2 sheath increases the lithium-storage capacity of CNTs by a factor of 3.

Figure 3c compares the rate performances of acid-treated CNTs before and after TiO_2 coating with the CNT-free TiO_2, whereby current densities of up to 5000 mA g^{-1} have been employed. Excellent rate capability is observed for the CNT@TiO_2 nanocomposite compared with both pure CNT and pure TiO_2. The specific capacity of CNT@TiO_2 can still maintain about 90% (from 265 mA h g^{-1} to 238 mA h g^{-1}) of its total capacity, whereas the current density increases from 800 mA g^{-1} to 5000 mA g^{-1}, whereas the value is only about 30% (from 201 mA h g^{-1} to 62 mA h g^{-1}) for the CNTs before TiO_2 coating, and nearly no capacity (less than 5 mA h g^{-1}) is observed for the CNT-free TiO_2 under these current densities. We are not aware of such a good performance for CNTs and TiO_2-based materials at these high rates in the literature. The connection between total specific capacity ($\tilde{C}$, i.e., total capacity per total mass) and individual specific storage capacities (partial capacity per partial mass) is given by $\tilde{C}_{\text{total}} = w_{\text{TiO}_2}\tilde{C}_{\text{TiO}_2} + w_{\text{CNT}}\tilde{C}_{\text{CNT}}$ with w being the mass fraction. As $\tilde{C}_{\text{CNT}}$ is larger than $\tilde{C}_{\text{TiO}_2}$, we have to strive for a low mass fraction of TiO_2 with the lower limit that the symbiotic function is not lost. In principle, the capacity of CNT@TiO_2 nanocomposite in the voltage windows of 1−3 V and 0.01−1 V can be roughly decomposed into the storage capacities of TiO_2 sheath ($\tilde{C}_{\text{TiO}_2}$) and CNT core ($\tilde{C}_{\text{CNT}}$), respectively. It was found that both the specific capacity in the CNT core (calculated on the basis of the only mass of CNT of the nanocomposite) and that in the TiO_2 sheath (calculated based on the only mass of TiO_2 of the nanocomposite) are much higher than that of the TiO_2-free CNT and that of the CNT-free TiO_2 sample, respectively (Figure 3c). These results demonstrate the synergism of the two cable wall materials.

Another excellent property of the CNT@TiO_2 nanocables is their excellent cycling performance. There is nearly no specific capacity loss over 100 cycles at a current density of 1000 mA g^{-1} (Figure 3d). The stable cycling properties imply that the chemical/mechanical robustness of the nanocomposite, which will be discussed in detail in the following. The Coulombic efficiency (calculated from the charge capacity/discharge capacity) of the CNT@TiO_2 composite is 94% in the first cycle under 1000 mA g^{-1} and always stabilize at 99−100% after the first cycle (see the inset in Figure 3d). The results also imply that the novel coaxial nanocable of CNT@TiO_2 is a robust structure and is very effective on improving the cycling performance. It is worth noting that the CNT@TiO_2 nanocomposite shows quite good contact with carbon black to form a robust mixed-conducting 3D networks on microscale level (see the Supporting Information, Figure S11). To confirm the improved electronic conductivity after introducing CNT into

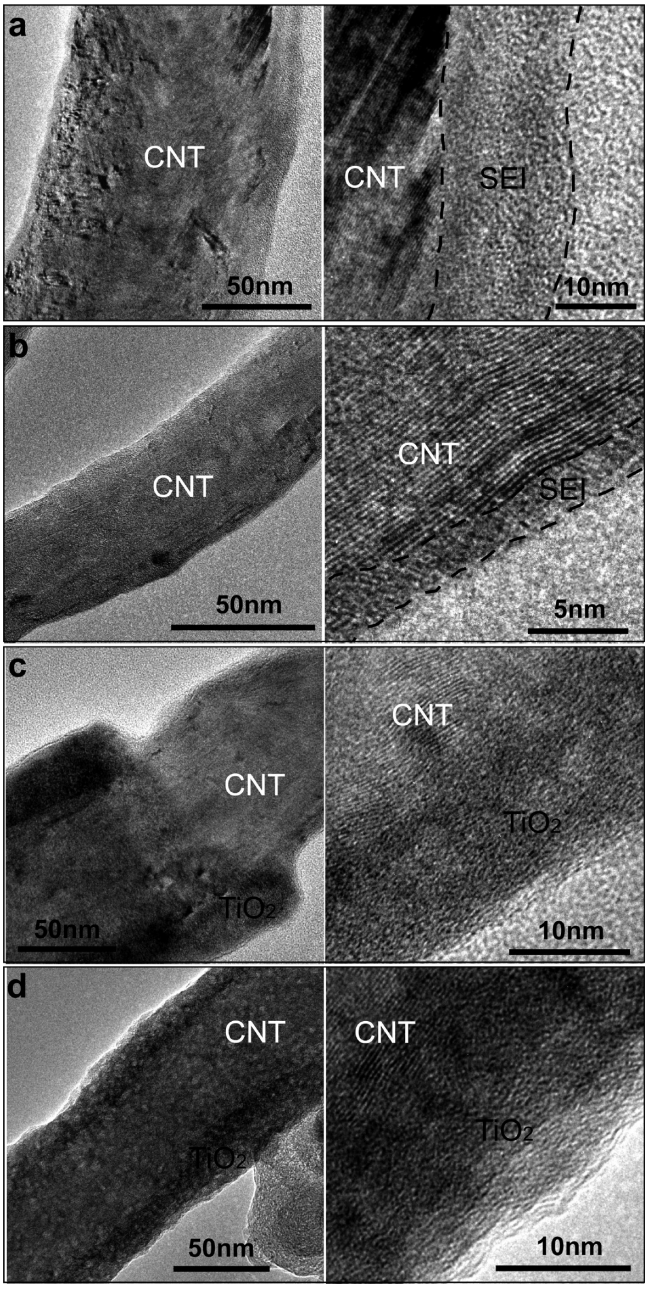

Figure 4. Characterization of surfaces. TEM images of bare CNTs in (a) a fully lithiated state and (b) a fully delithiated state. (c) CNT@TiO_2 nanocables in a fully lithiated state and (d) a fully delithiated state after 10 discharge/charge cycles under a current density of 3000 mA g^{-1}.

TiO_2, we measured the electronic conductivity of the TiO_2 and the CNT@TiO_2 nanocomposite. It was found that the overall electronic conductivity of the composite (ca. 0.001 S/m) is enhanced by as much as 4 orders of magnitude compared to that of the TiO_2 nanoparticles (ca. 1×10^{-7} S/m), demonstrating the improved electron transport due to the CNT cores.

Although the beneficial effect of CNT with respect to the Li storage in TiO_2 needs no further investigation, the beneficial role of TiO_2 for the Li storage in CNT requires a deeper understanding. For this purpose, the acid-treated CNTs before and after TiO_2 coating were investigated by HRTEM after ten discharge/charge cycles under a current density of 3000 mA g^{-1}. Figure 4 shows the

HRTEM images of the CNTs and CNT@TiO_2 nanocables in both fully lithiated (discharge) and fully delithiated (charge) states. The one-dimensional morphology of the two materials remained unchanged during the discharge/charge cycles in both states. For the bare CNTs, the thickness of as-formed SEI layer is up to 20 nm in the fully lithiated state (Figure 4a), whereas it is only 2 nm in the delithiated state (Figure 4a,b), indicating the unstable nature of the surface of CNTs toward SEI layer formation. However, only a very tiny SEI layer (ca. 1 nm) was found on the surface of TiO_2-coated CNTs in both states. It is thermodynamically required that SEI layers form at low voltage (generally below 0.8 V vs Li^+/Li) because of the electrolyte being reduced on the surface of the anode materials, yet the structure, composition, and thickness depend on the surface where it forms. Thick and unstable SEI layers not only consume active materials and cause large irreversible capacity losses (i.e., low Coulombic efficiency) as well as poor cycle life, they also hinder Li^+ transport and lead to low rate performance of electrodes.[28] Therefore, electrode materials without SEI or with very thin SEI layers are highly desired. (Note that for SEI the electronic and not the ionic conductivity limits the growth, so that the very thin SEI layer can be expected to be very easily crossed by ions.)[5] The very small thickness of the SEI is certainly also a key factor that, together with the easy pore transport of Li^+ from the electrolyte within the nanoporous sheath, guarantees quick Li^+ access for lithium storage in the CNT cores. The rate limiting step in the CNT@TiO_2 coaxial nanocables could be attributed to the lithium diffusion kinetics in CNTs and/or TiO_2 walls based on the above discussion. However, the reason for the tiny thickness of the SEI layer is not clear, it may be consequence of the composite structure, the large curvature of the pores, or the presence of a very thin TiO_2 layer (separating the pore structure from the CNT), which would be easily permeable by Li^+.

Conclusions

In summary, our results demonstrate that very effective synergism could be introduced by using two-phase structures such as the coaxial nanocables reported here. They can be used for designing superior electrode materials with improved performance in terms of power (rate), energy, and cycling behavior. The cable morphology also allows for a dense packing of electroactive materials. In addition to the bifunctionality on the nanoscale, it can easily form a micrometer-scale mixed-conducting network with carbon black as well. In the specific case of CNT@TiO_2 core/porous-sheath coaxial nanocable, on one hand, the benefit of CNT for TiO_2 storage consists in the electronic wiring principle (i.e., the CNT core providing sufficient e^- for the TiO_2 sheath). On the other hand, the benefit of nanoporous TiO_2 for CNT is the almost unperturbed Li^+ supply for the CNT core, most probably because of the porosity and the small thickness of the passivation layer. It is the synergism of the two parts that leads to a high, fast and stable lithium storage material. The strategy is simple, yet very effective; because of its versatility, it may also be extended to other electrode materials for future electrochemical energy storage devices[40] (LIBs, supercapacitors, or hybrid) combining high-power and high-energy densities.

Acknowledgment. This work is supported by the National Natural Science Foundation of China (Grants 50730005, 20821003, and 20701038), National Key Project on Basic Research (Grants 2006CB806100 and 2009CB930400), the Chinese Academy of Sciences, and the Max Planck Society. The authors thank Prof. Hong Li for useful discussions.

Supporting Information Available: Synthesis parameters for the CNT@TiO_2-precursors, SEM images of MWCNTs before and after treatment with HNO_3, XRD patterns and Raman spectra of the samples, SEM images of CNT@TiO_2-precursors, Nitrogen adsorption/desorption isotherms of MWCNTs before and after treatment with HNO_3, TGA of CNT@TiO_2 nanocables, SEM images and XRD pattern of TiO_2 sample synthesized under the control experiment in the absence of CNTs, galvanostatic discharge/charge curves in the voltage range of 0.01−3 V, and SEM images of CNT@TiO_2 nanocables before and after use in lithium batteries (PDF). This material is available free of charge via the Internet at http://pubs.acs.org.

(40) Simon, P.; Gogotsi, Y. *Nat. Mater.* **2008**, *7*, 845–854.